THE EFFECT OF FLAT SHAFT ON THE UNSTABLE VIBRATIONS OF A SHAFT CARRYING AN UNSYMMETRICAL ROTOR

(Part II. Experimental treatment)

Toshio YAMAMOTO, Hiroshi ŌTA and Kazutoyo KŌNO

Department of Mechanical Engineering

(Received October 13, 1969)

1. Introduction

The analytical treatments of this title are already reported in part I[1]. In this paper (part II), the experimental apparatus and results are shown mainly. The experimental results through four kinds of the shaft system agree well with the analytical results and they verify the conclusions (2) and (3) given in part I[1].

2. Experimental apparatus

Experiments are performed using experimental apparatus shown in Table 1. In Experiment I, the experimental apparatus consists of the vertical shaft of length $l=504.5$ mm with unsymmetrical stiffness supported by ball bearings at both the upper and lower shaft ends and the unsymmetrical rotor having $i_p \fallingdotseq 2$ and $\Delta=0.3041$. The length a between the lower shaft end and the rotor is 121.0 mm, and hence the length b between the upper end and the rotor is 383.5 mm.

TABLE 1. Dimensions of Experimental Apparatus

		Experiment I	Experiment II	Experiment III	Experiment IV
W	kg	10.433	11.894	13.681	12.179
I_p	kgcm s²	2.1790	0.4300	0.5512	0.3725
I	kgcm s²	1.0935	0.5276	0.6072	0.4943
ΔI	kgcm s²	0.3325	0.0637	0.1059	0.0446
α	kg/cm	3.3617×10^2	0.2659×10^2	0.2659×10^2	0.2659×10^2
$-\gamma$	kg/rad	3.5773×10^3	0.5456×10^3	0.5456×10^3	0.5456×10^3
δ	kgcm/rad	6.2036×10^4	1.4993×10^4	1.4993×10^4	1.4993×10^4
$\Delta\alpha$	kg/cm	0.1945×10^2	0.0274×10^2	0.0274×10^2	0.0274×10^2
$-\Delta\gamma$	kg/rad	0.1838×10^3	0.0480×10^3	0.0480×10^3	0.0480×10^3
$\Delta\delta$	kgcm/rad	0.4258×10^4	0.1169×10^4	0.1169×10^1	0.1169×10^4
$\sqrt{\alpha g/W}$	rpm	1697.0	446.9	416.9	441.9
$\sqrt{Ig/W}$	cm	10.135	6.593	6.595	6.307
i_p		1.9927	0.8150	0.9079	0.7536
δ		1.7966	12.9729	12.9665	14.1786
$-\gamma$		1.0499	3.1123	3.1108	3.2525
Δ		0.3041	0.1207	0.1744	0.0903
Δ_{11}		0.0579	0.1032	0.1032	0.1032
Δ_{12}		0.0514	0.0880	0.0880	0.0880
Δ_{22}		0.0686	0.0780	0.0780	0.0780

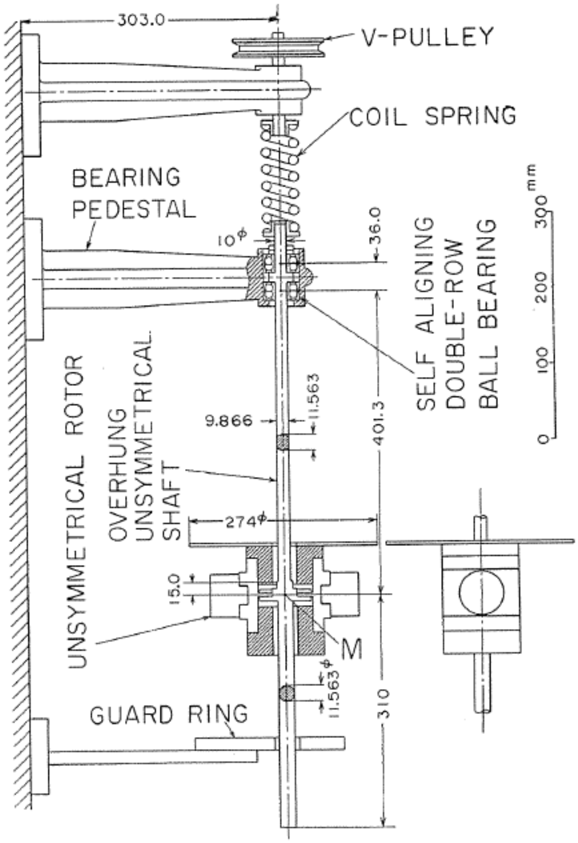

FIG. 1. Experimental apparatus (Experiment II, III and IV)

As shown in Table 1, the shaft used in Experiment I has unequal stiffness, *i.e.* $\Delta_{11} \fallingdotseq \Delta_{12} \fallingdotseq \Delta_{22}$. In Experiments II, III and IV, as shown in Fig. 1, the vertical shaft of length $l=401.3$ mm with unequal stiffness is supported by ball bearings only at the upper shaft end and the unsymmetrical rotor with $i_p<1$, $\Delta=0.1207$ (Experiment II) or $\Delta=0.1744$ (Experiment III) or $\Delta=0.0903$ (Experiment IV) is mounted at the free lower shaft end. In the upper shaft end the shaft are supported by two ball bearings equiped at a distance of $l_0=36.0$ mm. Ball bearings used in Experiments I, II, III and IV are the type of self-aligning double-row ball bearing with 10ϕ bore of #1200. All spring constants in Table 1 are calculated by beam theory.

3. Forced vibrations and static unstable region

In Fig. 2 the response curves of Experiment I in the neighborhood of the lower major critical speed ω_{c2} are shown in case of $\zeta=0°$ and $\zeta=90°$ by the symbol ○ and ● respectively. In case of $\zeta=0°$ the width of unstable region $2|\xi_0|$ is 1382 rpm−1146 rpm=236 rpm, and there is no unstable region in case of $\zeta=90°$. The width $2|\xi_0|$ near ω_{c2} obtained by Experiments I, II, III and IV are plotted against the orientation ζ in Figs. 3 (a), (b), (c) and (d) where the approximate

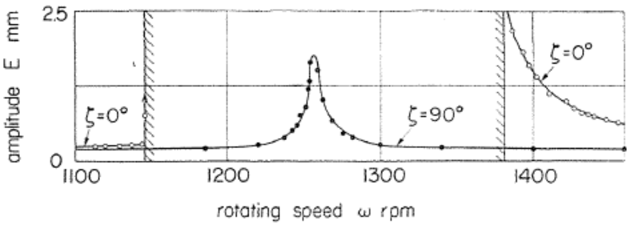

FIG. 2. Response curves at ω_{c2} in Experiment I.

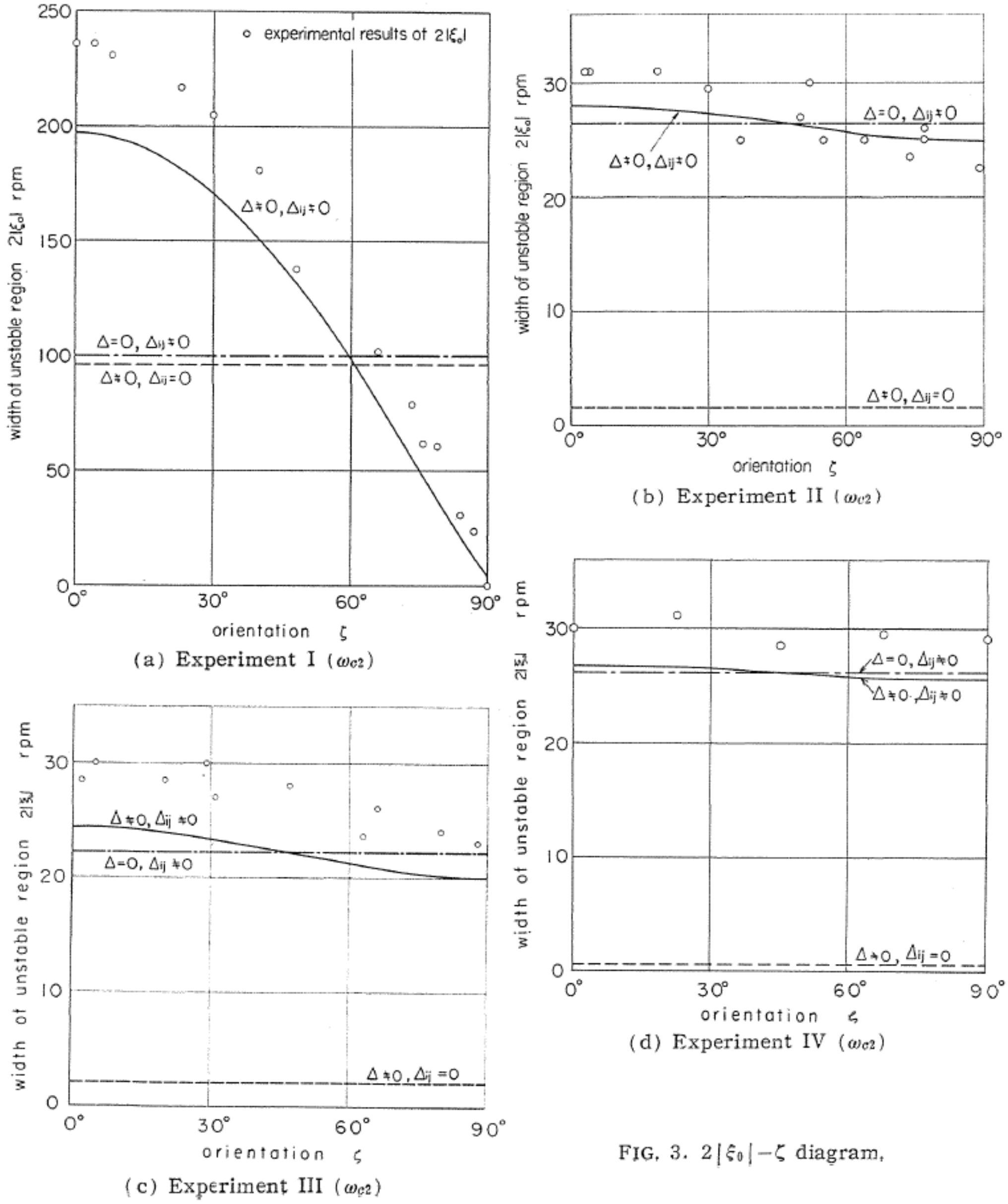

FIG. 3. $2|\xi_0|-\zeta$ diagram.

results through Eq. (16·a) and the experimental results are shown by full line curves and the symbols ○ severally; the calculated results when $\Delta=0$, $\Delta_{ij}\neq0$ and $\Delta\neq0$, $\Delta_{ij}=0$ of Experiments I, II, III and IV are added by chain and broken lines separately. It is seen from Eq. (16·a) given in Part I that in Experiment I the widths $2|\xi_0|$ when $\zeta=0°$ and $\zeta=90°$ are approximately equal to 197.3 rpm and 4.6 rpm respectively. Since in Experiment II, III and IV θ_x, θ_y are smaller than x, y in the neighborhood of ω_{c2}, the effect of inertia asymmetry Δ induced by the motions of θ_x, θ_y is also smaller than that of stiffness asymmetry Δ_{ij}, and hence the broken line of case $\Delta\neq0$, $\Delta_{ij}=0$ locates remarkably lower than the chain line of case $\Delta=0$, $\Delta_{ij}\neq0$, and further the simultaneous effect of Δ and Δ_{ij} becomes somewhat small as shown in Figs. 3 (b), (c) and (d). Through Experiments I, II, III and IV, QR takes positive value in the neighborhood of the lower major critical speed ω_{c2}.

Figs. 4 (a), (b) show the four natural frequencies p_{10}, p_{20}, $\bar{p}_{30}$ and $\bar{p}_{40}$ of free vibration when $\omega=0$, against the orientation ζ with experimental and analytical results which are denoted by ○ ⊖ ◒ ◓ and full-line curves, respectively. The difference between two natural frequencies p_{20}, $\bar{p}_{30}$ and the difference between p_{10}, $\bar{p}_{40}$ increase with ζ and take maximum values at $\zeta=90°$. This fact is in contrary to the width of the unstable region at major critical speed ω_c, for case of $\gamma=0$ or case of the flat uniform shaft ($\Delta_{ij}=\Delta s$).

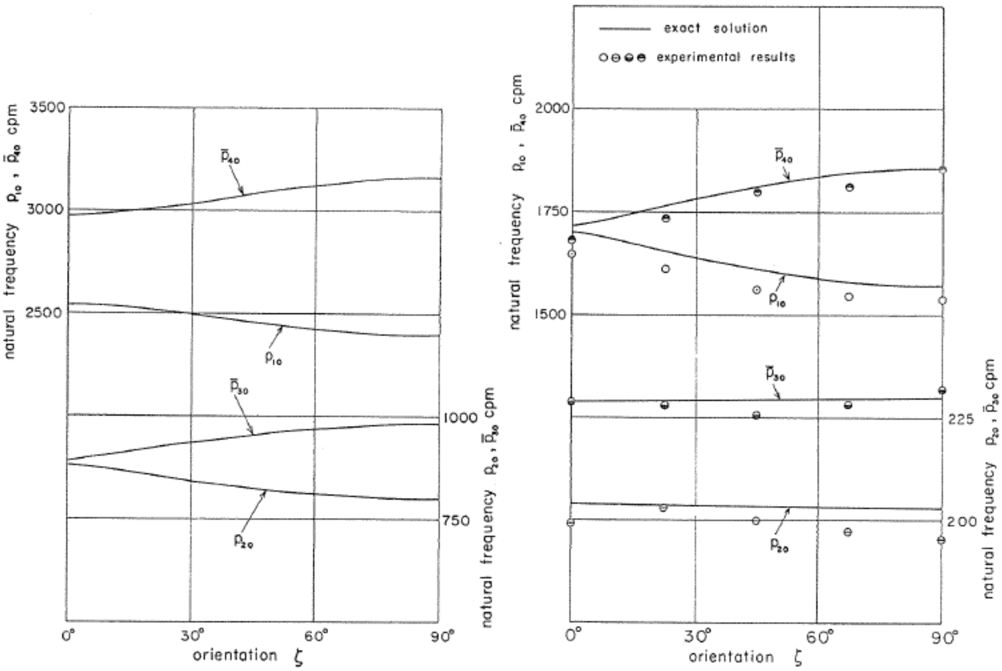

(a) Experiment I ($\omega=0$) (b) Experiment IV ($\omega=0$)

FIG. 4. p_{i0}, $\bar{p}_{i0}-\zeta$ diagram.

4. Free vibrations and dynamic unstable region

Though the dynamic unstable region does not appear in Experiment I because of $i_p \doteqdot 2$, in Experiment II, III, IV there are unstable regions near $\omega = \omega_d = 1216$ rpm, 1205 rpm, 1190 rpm respectively.

In Experiment II, IV for various values of ζ experimental and analytical results of the negative damping coefficient m are denoted by ● and full-line curves in Figs. 5 (a), (b), respectively. The actual unstable regions come slightly lower than

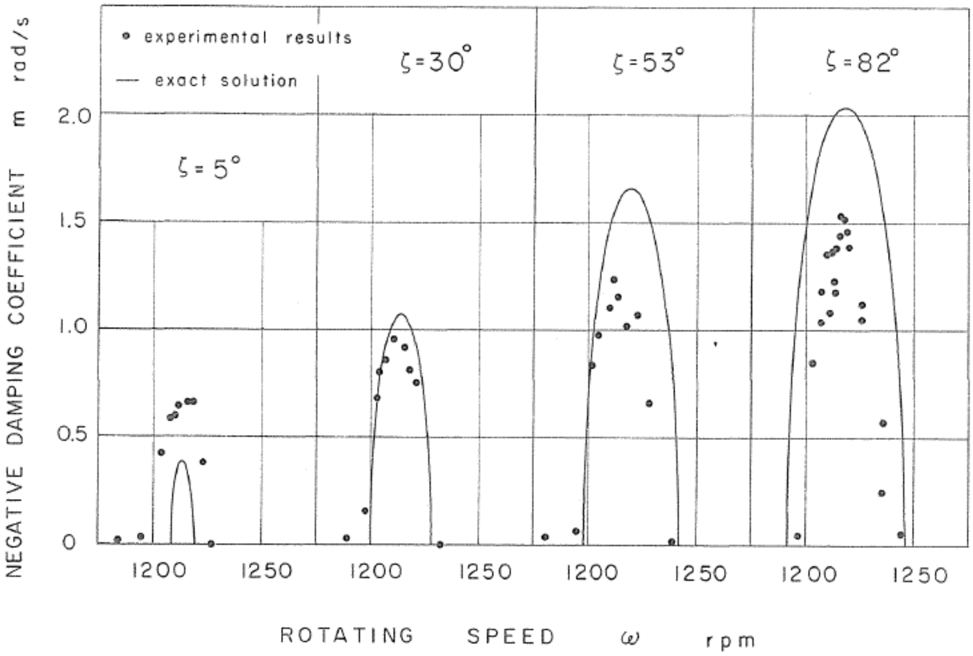

FIG. 5. (a) $m-\omega$ diagrams for $\zeta=5°$, 30°, 53° and 82° (Experiment II, ω_d)

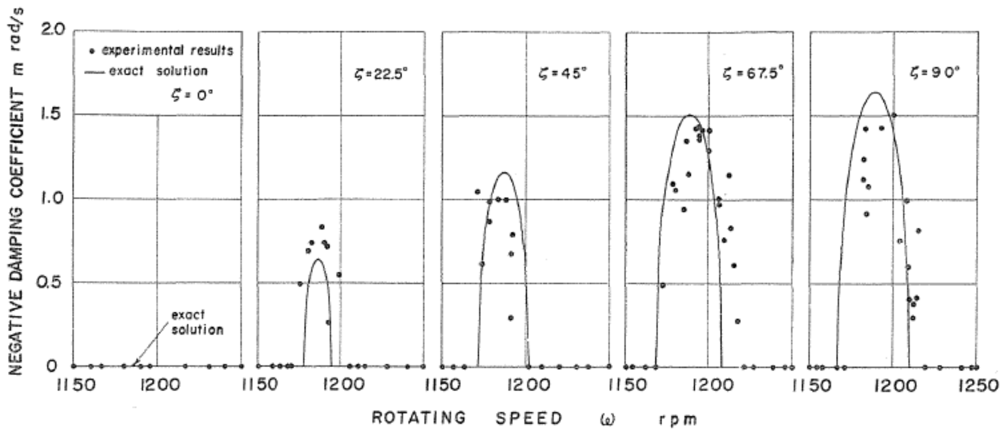

FIG. 5. (b) $m-\omega$ diagrams for $\zeta=0°$, 22.5°, 45°, 67.5° and 90° (Experiment IV, ω_d)

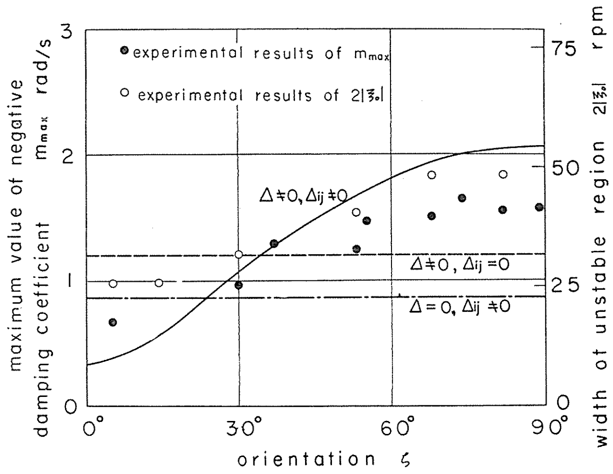

(a) Experiment II (ω_d)

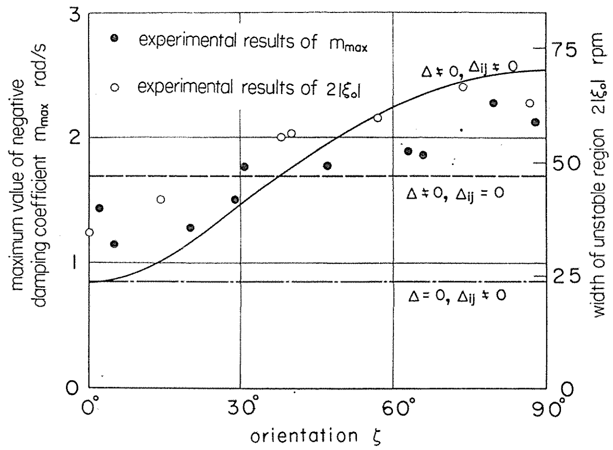

(b) Experiment III (ω_d)

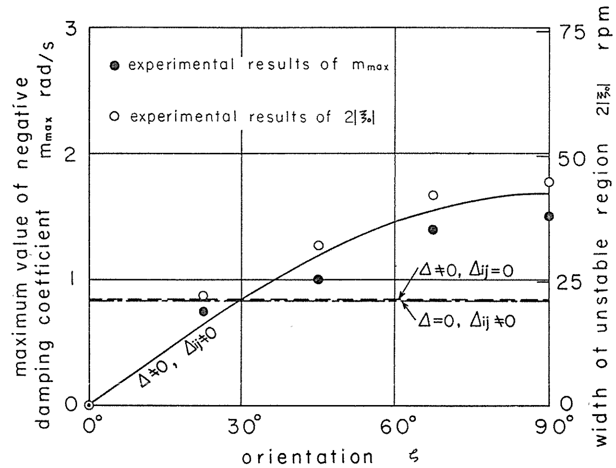

(c) Experiment IV (ω_d)

FIG. 6. m_{max}, $2|\xi_0|-\zeta$ diagram.

the analytical values because a massless shaft was assumed. Therefore, the latter is shifted to the lower side by 10 rpm (II), by 37 rpm (IV) in Figs. 5 (a), (b), respectively. The magnitudes of m and $2|\xi_0|$ increase with the orientation ζ. The approximate results of m_{max} and $2|\xi_0|$ through Eqs. (15・a), (16・a) are shown in Figs. 6 (a), (b) and (c) for Experiments II, III and IV where an appropriate scales are adopted so that the magnitudes of both m_{max} and $2|\xi_0|$ can coincide each other, because the magnitude of m_{max} is in proportion to that of $2|\xi_0|$. In Fig. 6, the symbols ● and ○ show the experimental results of m_{max} and $2|\xi_0|$ respectively. Further the approximate analytical results for cases $\Delta=0$, $\Delta_{ij}\neq 0$ and $\Delta\neq 0$, $\Delta_{ij}=0$ are added by chain and broken lines severally. In Experiments II, III and IV, $2|\xi_0|$ and m_{max} take their minimum and maximum values at $\zeta=0°$ and $\zeta=90°$ separately at ω_d because QR<0. Comparison between the analytical and experimental results is shown in Table 2 where the values in ( ) are the experimental results and $2|\xi_0|$ at ω_{c2} is the value at $\zeta=0°$ where it becomes maximum and m_{max}, $2|\xi_0|$ at ω_d is the value at $\zeta=90°$ where it takes maximum value.

TABLE 2. Comparison between Experimental and Analytical Results

			Experiment I	Experiment II	Experiment III	Experiment IV
Static unstable region	ω_{c2}	rpm	1228.8 (1256)	223.8 (220)	209.5 (209)	221.4 (219)
	$2\|\xi_0\|$ at $\zeta=0°$	rpm	197.3 (236)	28.0 (31)	24.3 (29)	26.7 (30)
Dynamic unstable region	ω_d	rpm		1228.4 (1216)	1197.0 (1205)	1227.2 (1190)
	m_{max} at $\zeta=90°$	rad/s		2.07 (1.6)	2.54 (2.3)	1.68 (1.5)
	$2\|\xi_0\|$ at $\zeta=90°$	rpm		54.1 (48)	70.3 (55)	41.9 (44)

Experimental results are shown in ( ).

The authors express their appreciation to Mr. K. Satō and Mr. T. Katō for their assistances.

Reference

1) T. Yamamoto, H. Ōta and K. Kōno, "The Effect of Flat Shaft on the Unstable Vibrations of a Shaft Carrying an Unsymmetrical Rotor" (Part I Analytical treatment), Memoirs of the Faculty of Engineering, Nagoya University, Vol. 21, No. 1 (1969), p. 122.